American Mineralogist, Volume 105, pages 1317–1325, 2020

Archean to Paleoproterozoic seawater halogen ratios recorded by fluid inclusions in chert and hydrothermal quartz

Ray Burgess[1,*,‡], Sarah L. Goldsmith[1], Hirochika Sumino[2], Jamie D. Gilmour[1], Bernard Marty[3], Magali Pujol[3,†], and Kurt O. Konhauser[4]

[1]Department of Earth and Environmental Sciences, University of Manchester, Manchester, M13 9PL, U.K.
[2]Department of Basic Science, Graduate School of Arts and Sciences, University of Tokyo, 3-8-1 Komaba, Meguro-ku, Tokyo, 153-0041, Japan
[3]Centre de recherches pétrographiques et géochimiques, CNRS, Université de Lorraine, 15, rue Notre-Dame-des-Pauvres, 54500 Vandoeuvre-lés-Nancy, France
[4]Department of Earth and Atmospheric Sciences, University of Alberta, Edmonton, Alberta T6G 2E3, Canada

Abstract

Past changes in the halogen composition of seawater are anticipated based on the differing behavior of chlorine and bromine that are strongly partitioned into seawater, relative to iodine, which is extremely depleted in modern seawater and enriched in marine sediments due to biological uptake. Here we assess the use of chert, a chemical sediment that precipitated throughout the Precambrian, as a proxy for halide ratios in ancient seawater. We determine a set of criteria that can be used to assess the primary nature of halogens and show that ancient seawater Br/Cl and I/Cl ratios can be resolved in chert samples from the 2.5 Ga Dales Gorge Member of the Brockman Banded Iron Formation, Hamersley Group, Western Australia. The values determined of Br/Cl ~2×10^{-3} M and I/Cl ~30×10^{-6} M are comparable to fluid inclusions in hydrothermal quartz from the 3.5 Ga North Pole area, Pilbara Craton, Western Australia, that were the subject of previous reconstructions of ancient ocean salinity and atmospheric isotopic composition. While the similar Br/Cl and I/Cl values indicate no substantial change in the ocean halide system over the interval 2.5–3.5Ga, compared to modern seawater, the ancient ocean was enriched in Br and I relative to Cl. The I/Cl value is intermediate between bulk Earth (assumed chondritic) and the modern seawater ratio, which can be explained by a smaller organic reservoir because this is the major control on marine iodine at the present day. Br/Cl ratios are about 30% higher than both modern seawater and contemporary seafloor hydrothermal systems, perhaps indicating a stronger mantle buffering of seawater halogens during the Archean.

Keywords: Halogen, argon isotopes, seawater salinity, chert, banded iron formation, ocean chemistry; Halogens in Planetary Systems

Introduction

There have been relatively few studies of halogens in the Archean oceans, and no reliable record of seawater halogen evolution has been compiled. In particular, past salinity changes in the oceans are largely unconstrained, and the biologically controlled evolution of the iodine cycle remains unknown. Previous studies have analyzed fluid inclusions to determine halogen ratios in Precambrian seawater. However several factors have hampered the interpretation of these results for understanding the halogen composition of the early oceans, including: the challenges of delimiting primary seawater composition in mixed hydrothermal fluids formed during seawater-basalt interaction processes; possible overprinting during later metamorphic and deformation events; and the analytical difficulties of determining low halogen concentrations, especially for least-abundant iodine.

The limited halogen data that exist are mainly derived from fluids associated with volcanic-sedimentary successions. This includes mid-Archean (~3.2 Ga) ironstone pods, and silicified komatiites and sediments from the Barberton Greenstone Belt, Kapvaal, South Africa (Channer et al. 1997; de Ronde et al. 1997; Farber et al. 2015); hydrothermal quartz in metabasalts from the ~3.4 Ga North Pole area, Pilbara, Western Australia (Foriel et al. 2004); and volcanic-related quartz veins and pods in the Paleoproterozoic (2.22 Ga) Ongeluk Formation, Kapvaaal, South Africa (Gutzmer et al. 2003).

Fluid inclusions in quartz veins hosted in ironstone pods from Barberton have chemical compositions that approximately match modern seawater, except for higher Br/Cl and I/Cl (de Ronde et al. 1997; Channer et al. 1997). These fluids may have been trapped fluids from seafloor hydrothermal vent systems (de Ronde et al. 1997), however both their age and origin is contested (de Ronde et al. 2004; Lowe and Byerly 2004), leading to uncertainty for their use in reconstructing early ocean chemistry (Lowe and Byerly 2003, 2007; Hren et al. 2006).

Crush-leach analysis of fluid inclusions in chert and quartz veins in komatiites from Barberton yielded Br/Cl and I/Cl much

* E-mail: ray.burgess@manchester.ac.uk. ORCID 0000-0001-7674-8718.
† Current address: TOTAL, Centre Scientifique et Techniques Jean-Féger, Pau, France.
‡ Special collection papers can be found online at http://www.minsocam.org/MSA/AmMin/special-collections.html.

0003-004X/20/0009–1317$05.00/DOI: https://doi.org/10.2138/am-2020-7238

higher than modern seawater and, although some overlap with the range reported by Channer et al. (1997), most are considerably higher, similar to those observed in organic-rich fluids (Farber et al. 2015) and also inclusion fluids present in minerals in rocks from Caledonides, western Norway (Svensen et al. 2001), perhaps indicative of a metamorphic overprint.

North Pole hydrothermal quartz contains several types of fluid inclusions with variable Br/Cl values that are 1–2 times modern seawater values (Foriel et al. 2004), and quartz-bearing fluid inclusions from the Onglevlauk Formation also have Br/Cl ratios ≥2 times the modern value (Gutzmer et al. 2003). In these studies, the elevated Br/Cl values are thought to reflect the influence of mantle-derived hydrothermal vent compositions, as there was likely insufficient organic matter present to fractionate Br from Cl toward the modern value. Only in settings isolated from the main oceans, such as in the lagoonal depositional environment proposed for the North Pole area, was there sufficient organic matter to decrease the Br/Cl ratio of seawater toward the modern value (Foriel et al. 2004).

Temporal changes in seawater Cl abundance (salinity) has also been a topic of interest, with suggestions that Precambrian oceans may have been between at least two times more saline than the modern value (Knauth 1998; Weiershäuser and Spooner 2005). Due to its formation in volcanic hydrothermal systems, quartz rarely contains primary seawater in fluid inclusions, making it difficult to reconstruct seawater salinity. However, Marty et al. (2018) used ^{36}Ar/Cl/K mixing relationships in fluids extracted from 3.4 Ga North Pole quartz to show that Archean seawater had comparable Cl salinity to modern oceans.

Martin et al. (2006) reviewed available evidence for Archean and Proterozoic seawater chemistry noting the similarity with Ca-Na-Cl and Na-Ca-Cl brines found in most Precambrian shields including Finland, Sweden, Russia, and Canada. They considered that the chemical composition of Archean seawater may have been comparable to modern seawater but was modified by water-rock interactions or contamination by hydrothermal fluids. A common finding of previous studies is that Archaean ocean water chemistry was strongly buffered by mantle input by emission of dissolved ions from mid-oceanic vents and high-temperature water-rock interactions in the oceanic crust (Martin et al. 2006).

The approach and rationale used in this study is outlined as follows. First, we have determined the halogen ratios (Cl, Br, I) in fluid inclusion-bearing hydrothermal quartz from the North Pole area. These samples have been the subject of several previous studies, in particular to determine their fluid compositions and Br/Cl ratios (Foriel et al. 2004), seawater salinity (Marty et al. 2018), and ancient atmospheric isotopic compositions of Ar, Xe, and N_2 (Pujol et al. 2011, 2013; Marty et al. 2013; Avice et al. 2018). Second, we analyzed halogens in cherts from the Dales Gorge Member of the Brockman Iron Formation, Hamersley Group, Western Australia. Chert in Banded Iron Formations (BIF) is considered to be an early diagenetic phase derived either from abiogenic amorphous silica or a siliceous Fe oxyhydroxide precursor phase. Silica precipitation occurred directly from Si-saturated seawater or via absorption of Si on Fe hydroxides (e.g., Morris 1993; Maliva et al. 2005; Posth et al. 2008). The microcrystalline nature of BIF chert means primary seawater is likely to be initially trapped between particles/colloids during deposition. Some of this fluid will subsequently be retained in intercrystalline porosity formed during diagenesis and dewatering. Fluid flow and particle redistribution in this microporous network has recently been considered by Egglseder et al. (2018) as a process that may lead to the formation of chert/iron-rich microbands. Cherts are widespread and common throughout the geological record and preserve the earliest fossils, single cell walls and filaments, e.g., those found in the 3.47 Ga old Apex Chert of Western Australia (Schopf et al. 2002). They also have low permeability and are resistant to later dissolution and reprecipitation, and even during metamorphic recrystallization water/rock ratios are usually so low that δ^{18}O is unaffected (Knauth and Lowe 2003). Cherts have been used to investigate the physical and chemical conditions in past oceans in numerous studies (reviewed by Konhauser et al. 2017), although not previously for halogens, so they are assessed here as an alternative record of seawater halogen ratios, independent from that obtained from hydrothermal quartz.

Third, we pay particular attention to the I/Cl value of seawater. Iodine has a much higher affinity for organic matter, potentially making it a potent indicator of the biological influences on ocean water chemistry. There has been only one previous estimate of the I/Cl ratio of Archean oceans of ~40×10^{-6} M (Channer et al. 1997), which is higher than present day value of 0.86×10^{-6} M (Li 1991). The biophilic behavior of I has led to suggestions that the iodine abundance of the oceans may have decreased over time in response to evolutionary changes (e.g., de Ronde et al. 1997; Hardisty et al. 2014). Changes in reservoir size of biologically related iodine in the oceans would also have impacted atmospheric chemistry because volatile organohalides influence the oxidative capacity of the atmosphere and can form ultrafine aerosol particles, which are important as cloud condensation nuclei and provide a major pathway for transferring marine iodine to the continents (e.g., Saiz-Lopez et al. 2011).

Finally, to overcome the analytical challenges related to samples containing low halogen abundances and mixed fluid compositions, we used the neutron-irradiation noble gas technique. This method has low halogen detection limits (<1 ppb I) and, because it combines halogens with noble gas isotope measurements, can be used to obtain a range of insights into fluid systems including their origin, temperature, salinity, and age (Turner et al. 1993; Ballentine et al. 2002). As such, it has been applied to a wide range of ancient fluid systems (e.g., Kelley et al. 1986; Tuner et al. 1993; Bohlke and Irwin 1992a; Kendrick et al. 2001; Ballentine et al. 2002).

Samples and geological setting

Quartz samples PI-02-39 and PI-06 are from the 3.5 Ga old Dresser formation, Warrawoona Group, Pilbara Craton at North Pole, Western Australia (Foriel et al. 2004). The Dresser Formation is a sedimentary-volcanic succession comprising pillowed metabasalts and metakomatiites interbedded with cherty metasediments and is interpreted to have formed in a hydrothermal system associated with a volcanic caldera (Van Kranendonk 2006). Both quartz samples analyzed are from a drill core (Pilbara Drilling Project 2) and were collected at between 102 and 110 m depth. PI-06-39 and PI-06 are from quartz-carbonate aggregates forming pods in centimeter-sized vacuoles in a metakomatiite (Buick and Dunlop 1990; Pujol et

al. 2011). The host rocks are undeformed and have experienced only low-grade metamorphism between 100–350 °C, probably occurring shortly after deposition 3.5 Ga ago (Terabayashi et al. 2003; Van Kranendonk 2006). Quartz contains abundant mixed aqueous-vapor fluid inclusions with variable salinity (average ~12 wt% NaCl) considered to be of primary origin (Foriel et al. 2004). The age of trapped fluids is likely >3.0 Ga, and probably contemporaneous with the Dresser formation (Pujol et al. 2013), they contain low atmospheric $^{40}Ar/^{36}Ar$ ratios ($^{40}Ar/^{36}Ar = 143 \pm 24$, 1σ) and isotopically fractionated xenon characteristic of Archean atmosphere (Pujol et al. 2011, 2013; Avice et al. 2018). The fluids are interpreted as being mixtures of seawater and two or more different hydrothermal end-member mixtures (Foriel et al. 2004). The hydrothermal end-members are rich in metals (Fe, Ba), Cl, K, and parentless ^{40}Ar (Foriel et al. 2004; Pujol et al. 2011). Marty et al. (2018) used noble gases released by crushing of neutron-irradiated samples of PI-06-39 and PI-06 to show that the salinity (Cl) of 3.5 Ga Archean seawater was comparable to modern seawater, with perhaps a 40% lower potassium abundance. Foriel et al. (2004) used the chemical composition to divide the fluid inclusions into three types, two hydrothermal fluids with Br/Cl of ~2.6×10^{-3} M, and a low Br/Cl fluid considered to be representative of seawater.

Nine samples were selected from different depths in the DDH44 drill core at Paraburdoo from the ca. 2.5 Ga Dales Gorge Member, Brockman Banded Iron Formation, Hamersley Group, Western Australia (Ewers and Morris 1981). Samples 36.7–13, 96.8–14, and 146.7/8 were available from the previous study by Hamade et al. (2003). The Dales Gorge Member is one of the best-preserved BIFs, and has been extensively studied to make inferences about ancient environmental conditions and biological processes (e.g., Trendall and Blockley 1970; Ewers and Morris 1981; Morris 1993; Krapež et al. 2003; Pecoits et al. 2009; Rasmussen et al. 2013, 2014). It is ~150 m thick and divided into 17 depositional sequences. The BIF macrobands are themselves composed of mesobands (millimeter to centimeter thick) apparent as alternating iron oxide-rich (hematite, magnetite) and chert-rich bands that are laterally continuous. Chert mesobands are, in turn, often characterized by fine microbands (sub-millimeter thickness), also defined by alternation of iron oxides and chert (Rasmussen et al. 2013). Chert is interpreted to have formed from amorphous silica, which either precipitated directly from the water column (Ewers and Morris 1981) or formed below the sediment-water interface as a diagenetic replacement (Krapež et al. 2003; Rasmussen et al. 2013, 2014). The Dales Gorge Member has undergone very low- to low-grade metamorphism and minor deformation (Smith et al. 1982; Kaufman et al. 1990). Based on textural evidence, the hematite present in iron-rich bands either formed by dehydration of ferric oxyhydroxides that precipitated in the water column (Sun et al. 2015) or by secondary replacement growth during the 2.2 Ga Ophthalmian Orogeny (Rasmussen et al. 2005). While the movement of hydrothermal fluids is thought to be responsible for the deposition of microplaty hematite, which forms the major ore bodies in the region (Brown et al. 2004), the samples in this study are generally considered primary in nature (Robbins et al. 2019).

Since BIFs are marine sediments, not associated with lavas or other igneous bodies, they are less likely to be directly influenced by hydrothermal systems. The Hamersley samples studied have positive Eu/Eu* anomalies between 1.3–2.4 and elevated but variable Y/Ho of 34–62 (data from Hamade 2002 and given in Table 1). On a Y/Ho–Eu/Eu* diagram (Fig. 1), they are intermediate between crust and Archean seawater values, the latter represented by data from the 3.40 Ga Strelley Pool Chert (Van Kranendonk et al. 2003). The lack of evidence for a hydrothermal end-member in Figure 1 indicates the cherts did not precipitate directly from hot fluids. On this basis, Hamersley samples precipitated at least partially to mostly from Archean seawater, possibly contaminated with crustal material.

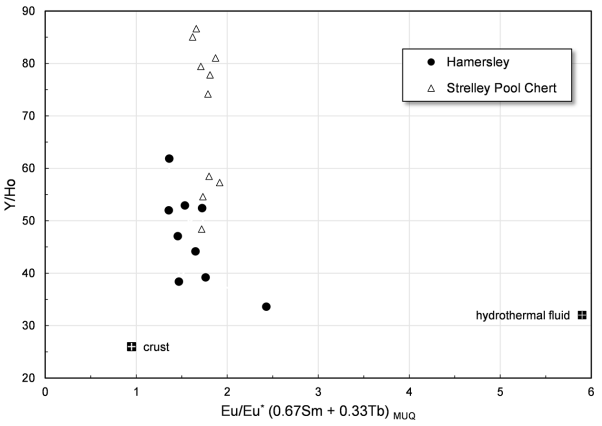

Figure 1. Y/Ho vs. Eu/Eu* ratio calculated as $Eu/[(0.67Sm + 0.33Tb)]_{MUQ}$. MUQ = average mud from Queensland (Kamber et al. 2005). End-member compositions for crust and hydrothermal fluids from Pinti et al. (2009). The Strelley Pool stromatolite data are considered to precipitate from Archean seawater (Van Kranendonk et al. 2003).

Table 1. Halogen data for Hamersley chert samples (1 St.dev. error)

Sample	Fe_2O_3[a] wt%	Hematite[a] wt%	Magnetite[a] wt%	Y/Ho[a]	Eu/Eu*[a]	T (°C)[b]	Cl (ppm)	% Cl release	Br/Cl (×10³)	I/Cl (×10⁶)	$^{36}Ar/Cl$ (×10⁻⁹)
36.7	61.9	21.2	27.3	1.364	61.9	1400	21.7 ± 0.1	47.7	1.94 ± 0.11	26.3 ± 0.6	74.7 ± 1.8
36.11	31.9	11.4	9.3	1.358	52.0	1400	14.2 ± 0.1	47.9	1.90 ± 0.02	32.4 ± 0.7	113.9 ± 1.9
36.12	59.5	23.7	14.3	1.535	52.9	1400	21.1 ± 0.2	45.3	2.04 ± 0.03	31.5 ± 2.6	95.5 ± 4.3
36.13	40.3	14.3	12.8	1.651	44.2	1600	14.3 ± 0.1	50.1	2.04 ± 0.01	30.2 ± 0.8	74.7 ± 2.3
96.8	34.0	17.7	12.4	1.469	38.4	1400	8.0 ± 0.1	43.4	1.97 ± 0.02	26.6 ± 1.0	84.9 ± 4.9
96.13	71.5	25.2	45.7	1.457	47.1	1600	16.9 ± 0.1	50.2	2.24 ± 0.01	28.7 ± 0.7	80.1 ± 2.5
96.14	53.3	11.4	26.7	1.726	52.4	1400	20.0 ± 0.1	46.3	2.06 ± 0.01	28.8 ± 0.8	74.0 ± 1.8
146.6	61.9	54.5	10.0	1.762	39.2	1400	18.2 ± 0.2	51.1	2.15 ± 0.02	20.3 ± 3.3	78.2 ± 1.5
146.7/8	45.6	28.7	4.4	2.429	33.6	1600	23.0 ± 0.1	59.1	1.84 ± 0.01	14.4 ± 0.4	55.8 ± 1.3

[a] From Hamade (2002); $Eu/Eu^* = Eu_{MUQ}/(0.67Sm + 0.33Tb)_{MUQ}$, MUQ = average mud from Queensland (Kamber et al. 2004).
[b] Temperature of the main halogen release during stepped heating.

Experimental methods

Hamersley samples were hand-picked under a binocular microscope to ensure only vein-free chert was analyzed, and then crushed to a coarse powder. North Pole samples were prepared as millimeter-sized chips. Halogens were determined using neutron irradiation noble gas mass spectrometry (Turner 1965; Bohlke and Irwin 1992b; Kendrick 2012; Ruzié-Hamilton et al. 2016). The samples were irradiated at the Safari-1 reactor, NECSA, South Africa, for 24 h to receive an integrated neutron dose of ~10^{19} n cm^{-2}. Noble gas isotopes $^{38}Ar_{Cl}$, $^{80}Kr_{Br}$, $^{128}Xe_{I}$, $^{39}Ar_{K}$, and $^{37}Ar_{Ca}$ are formed following neutron reactions with parent isotopes of Cl, Br, I, K, and Ca, respectively. Following irradiation, noble gases were released either by in vacuo crushing (North Pole samples) or by furnace heating (Hamersley samples). Sample crushing was carried-out using modified Nupro valves (Stuart et al. 1994), by loading 10–50 mg of sample into a crucible placed in the body of the valve. Prior to crushing, the samples were evacuated and baked at 250 °C for 12 h. Samples were progressively crushed in 5–6 steps by repeatedly lowering and raising the valve stem with a modified tip designed to crush the sample.

During furnace heating, approximately 20–50 mg of sample powder was wrapped in pure Al foil and placed into the "Christmas" tree loading device of the furnace. The resistance furnace is manufactured from Ta metal components, contained in a secondary vacuum chamber to prevent oxidation during heating. Samples were dropped into the furnace by externally manipulating an iron slug placed behind each sample, using a hand magnet. Temperatures were monitored using a thermocouple positioned at the base of the furnace tube. Samples were heated to between 400–1800 °C in 200 °C steps, each of 30 min duration.

Noble gases released either by crushing or stepped heating were purified using the same procedure: initially using a hot SAES G50 getter in close proximity to the furnace or crusher devices; then with a hot SAES ST171 getter positioned close to the inlet of the mass spectrometer; and finally with an SAES NP10 getter at room temperature mounted adjacent to the mass spectrometer ion source. Isotopic analyses were made using the MS1 mass spectrometer, a custom-built single focusing magnetic sector mass spectrometer equipped with a continuous dynode channeltron and a Faraday detector (Ruzié-Hamilton et al. 2016). Peak height determinations were made by switching the magnetic field over the mass range for Ar, Kr, and Xe isotopes (m/z 36–136), using nine measurement cycles. Baseline readings at intermediate masses were also measured and subtracted from peak readings. Following isotopic analysis, raw data were regressed to mass spectrometer inlet time, corrected for blanks (determined by heating an empty Al foil wrapping, or in the static volume of the crushers), neutron interferences, radioactive decay and mass discrimination (the latter only for Ar isotopes), and converted to moles using calibrated volumes of air standard, analyzed daily during the period of the experiments. Methods used for converting neutron-produced noble gas isotopes to parent halogen, K, and Ca concentrations follow those described by Ruzié-Hamilton et al. (2016). Reported elemental ratios are in molar (M) units and uncertainties are one standard deviation unless otherwise stated.

Results and discussion

Data obtained from crushing and stepped heating are summarized in Table 1 and the full data set is available in Supplemental[1] Table S1. Data for the Hamersley samples do not show any correlation, or systematic differences, with sampling depth, mesoband mineralogy or Fe content (Table 1). For this reason, results obtained from different samples are not differentiated in the following discussion. Furthermore, in assessing the sample data for the presence of ancient seawater we make the same conservative assumptions of previous studies (Turner 1989; Pujol et al. 2013; Marty et al. 2018), that during the Archean the partial pressure of ^{36}Ar in the atmosphere was similar to today, and that ^{36}Ar concentrations in seawater are a primarily a function of temperature and salinity only.

Retention of a primary seawater halogen signature in chert

Stepped heating noble gas release patterns are similar for all chert samples. There are two main gas releases: (1) a fairly broad release between 600–1000 °C, representing the predominant release for $^{37}Ar_{Ca}$ (57–89%) and $^{39}Ar_{K}$ (44–78%); and (2) a sharp release occurring at either 1400 or 1600 °C, normally corresponding to the main release of $^{38}Ar_{Cl}$ (43–59%); $^{80}Kr_{Br}$ (41–69%) and $^{128}Xe_{I}$ (55–78%).

The stepped release pattern indicates that halogens are hosted by at least two different phases in chert. The host(s) of the lower temperature release (600–1000 °C) is not known with certainty, but possible candidates include iron oxides that are able to adsorb halide ions or carbonate minerals, the latter implicated by the large $^{37}Ar_{Ca}$ release. Cherts are also known to contain noble gases dissolved in a fluid phase and, during previous stepped heating studies of irradiated cherts, this component has been shown to be retained until >1200 °C (Turner 1988). Further insights into the nature of the phase(s) releasing most of the halogen-derived noble gases at high temperature can be gained by considering the K-Ar-Cl relationships below.

K-^{40}Ar age constraints

Figure 2a shows a plot of K/^{36}Ar vs.^{40}Ar/^{36}Ar for heating steps from all samples, and Figure 2b shows data for high-temperature steps only (1200–1600 °C). The low temperature stepped heating

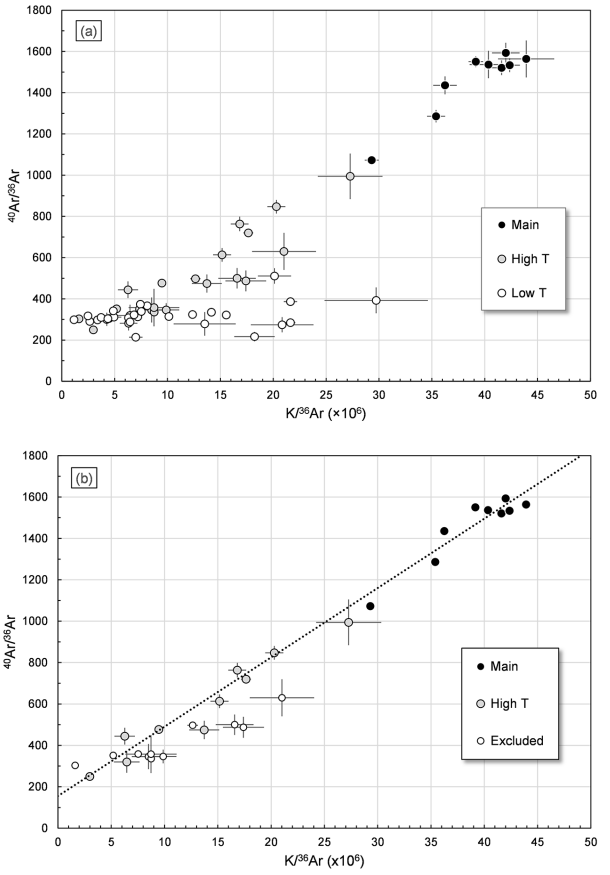

Figure 2. ^{40}Ar/^{36}Ar vs. K/^{36}Ar plot for 9 chert samples from Dales Gorge Member, Brockman BIF, Hamersley Group, Western Australia. (**a**) Low *T* refers to heating steps 600–1000 °C; High *T* are steps at 1200–1600 °C; and Main is the dominant release step for K-derived ^{39}Ar at either 1400 or 1600 °C (**b**) High temperature and Main release steps only, additionally the 1200 °C step for each sample is excluded from the regression. The line of best fit (dotted) yields a slope ^{40}Ar*/K = (33.68 ± 1.3) × 10^{-6} and an intercept ^{40}Ar/^{36}Ar = 142 ± 31 (2σ errors).

data show a limited range of $^{40}Ar/^{36}Ar$ values (216–400), and do not correlate with $K/^{36}Ar$ (Fig. 2a). In contrast, high-temperature data form a reasonable linear relationship (Fig. 2b) indicating that ^{40}Ar is composed of a mixture between a K-poor, low $^{40}Ar/^{36}Ar$ (<250) end-member, and a K-rich, radiogenic ^{40}Ar end-member. The best fit line shown in Figure 2b was obtained by linear regression of the data obtained for steps above >1200 °C. The 1200 °C steps were excluded from the fit because some show evidence of mixing with the low-temperature component, these data are indicated in Figure 2b. The slope of the best-fit line corresponds to an age of 2383 ± 183 Ma (2σ) with an intercept $^{40}Ar/^{36}Ar$ of 142 ± 31 (MSWD = 1.6, p = 0.07). The linear regression is not considered to be a robust isochron because, even after excluding the 1200 °C step from the regression, it is possible that some residual gas is being released from the low temperature phase. Furthermore, the K-bearing phase is likely to be fine-grained, making ^{39}Ar recoil into surrounding chert a strong possibility. Nevertheless, the age obtained is consistent with both the timing of hydrothermal vein formation in the Dales Gorge Member, considered to be related to the ca. 2.2 Ga Ophthalmian Orogeny (Brown et al. 2004), and the age of 2461 ± 6 Ma determined by U-Pb dating of zircons from an ash-fall tuff in macroband S13 (Trendall et al. 2004). The trapped $^{40}Ar/^{36}Ar$ value of 142 ± 31 is lower than modern atmosphere (296) and within error of the palaeo-atmospheric $^{40}Ar/^{36}Ar$ composition of sample PI-06 from the 3.4 Ga Dresser Formation of 143 ± 24 (Pujol et al. 2011). In summary, the high temperature release of Ar from Hamersley cherts is consistent with the presence of a ~2.4 Ga old K-bearing phase preserving an ancient atmospheric component.

Salinity of the trapped fluid released at high temperature

Hamersley heating data are shown on a plot of $Cl/^{36}Ar$ vs. $K/^{36}Ar$ in Figure 3, where it can be seen that there is a general positive correlation. Notably, the main release steps (at 1400 or 1600 °C) from each sample have $Cl/^{36}Ar$ values comparable to modern seawater salinity in the temperatures range 0–25 °C (calculated from equations in Hamme and Emerson 2004). This is similar to the finding of Marty et al. (2018) for North Pole fluids, which are also shown for comparison in Figure 3. However, $K/^{36}Ar$ of the Hamersley high temperature steps are about two orders of magnitude higher than modern seawater. This can be explained by the presence of a K-rich phase yielding the ~2.3 Ga age discussed earlier and implies that both sold and fluid inclusions are co-released during melting of the host chert. The fluid phase is likely to be paleo-seawater containing dissolved atmospheric noble gases based on the low $^{40}Ar/^{36}Ar$ ratio, seawater-like $Cl/^{36}Ar$ ratios, and the ~2.4 Ga ^{40}Ar-^{39}Ar age.

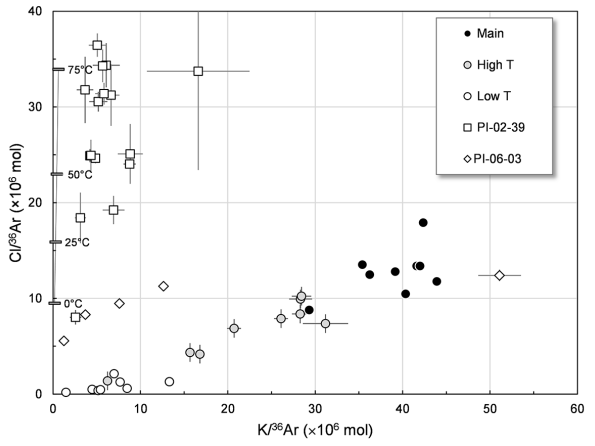

Figure 3. $Cl/^{36}Ar$ vs. $K/^{36}Ar$ data obtained by stepped heating of Hamersley chert and in vacuo crushing of North Pole (PI) quartz samples. Hamersley data are subdivided on the basis of low T = temperature steps between 600–1000 °C; High T = steps between 1200–1600 °C, and Main release at either 1400 or 1600 °C. Data from individual crushing steps are shown for North Pole samples. The solid line represents modern seawater salinity over the temperature range 0–75 °C calculated using equations from Hamme and Emerson (2004).

Fluid inclusions present in North Pole quartz are comprised of three fluid types having different salinities and metal composition (Foriel et al. 2004). The slightly elevated $Cl/^{36}Ar$ values obtained by crushing (Fig. 3) may reflect their hydrothermal origins, and the lower $K/^{36}Ar$ values compared to cherts indicates either an absence of a K-rich phase, or that this component is not released during crushing.

Halogen ratios of fluid inclusions

Br/Cl and I/Cl vs. $^{36}Ar/Cl$ is shown for chert samples in Figure 4. Low-temperature heating steps give highly variable $^{36}Ar/Cl$ values, and do not show any correlations (Fig. 4a). The variability in $^{36}Ar/Cl$ ratios of the low-temperature release steps is attributed to the presence of a ^{36}Ar-bearing component in the samples, most likely modern air contamination, as indicated by their air-like $^{40}Ar/^{36}Ar$ ratios (Fig. 2). The high temperature (>1200 °C) steps give lower and more consistent $^{36}Ar/Cl$ values indicative of a single fluid component having a relatively uniform composition similar to that observed in the North Pole quartz samples (Fig. 4b). Assuming the main release step is representative of ~2.5 Ga seawater as discussed earlier, then $Br/Cl = (2.02 \pm 0.13) \times 10^{-3}$ M and $I/Cl = 26.6 \pm 5.8 \times 10^{-6}$ M, which are about 30% and 30 times higher than the present-day seawater values, respectively.

While the process of formation remains unknown for Hamersley BIF cherts, the main control on halogen fractionation does not appear to be related to the depositional processes causing mineralogical banding in the cherts (Table 1). Retention of halogen variations on the centimeter-scale further supports the view that cherts provide a reliable record of fluid compositions over long geological timescales.

Hamade et al. (2003) suggest that banding in the Dales Gorge Member is controlled by the varying influence of continental vs. hydrothermal inputs to the basin. Br/Cl and I/Cl of modern continental runoff is variable (e.g., Moran et al. 2002; Tagami and Uchida 2006) but mostly exceeds modern seawater and mantle ratios. Thus, it is possible that the relatively minor intersample variations result from changing fluxes of halogens from the basin, although there is no evidence for mixing relationships in our data or relationship with REE ratios (Fig. 1, Table 1) that may support the presence of these two end-members.

Changes in composition at the mesoband scale are also unlikely to be caused by fluctuations in the source because deposition rate is much shorter than the residence time of any

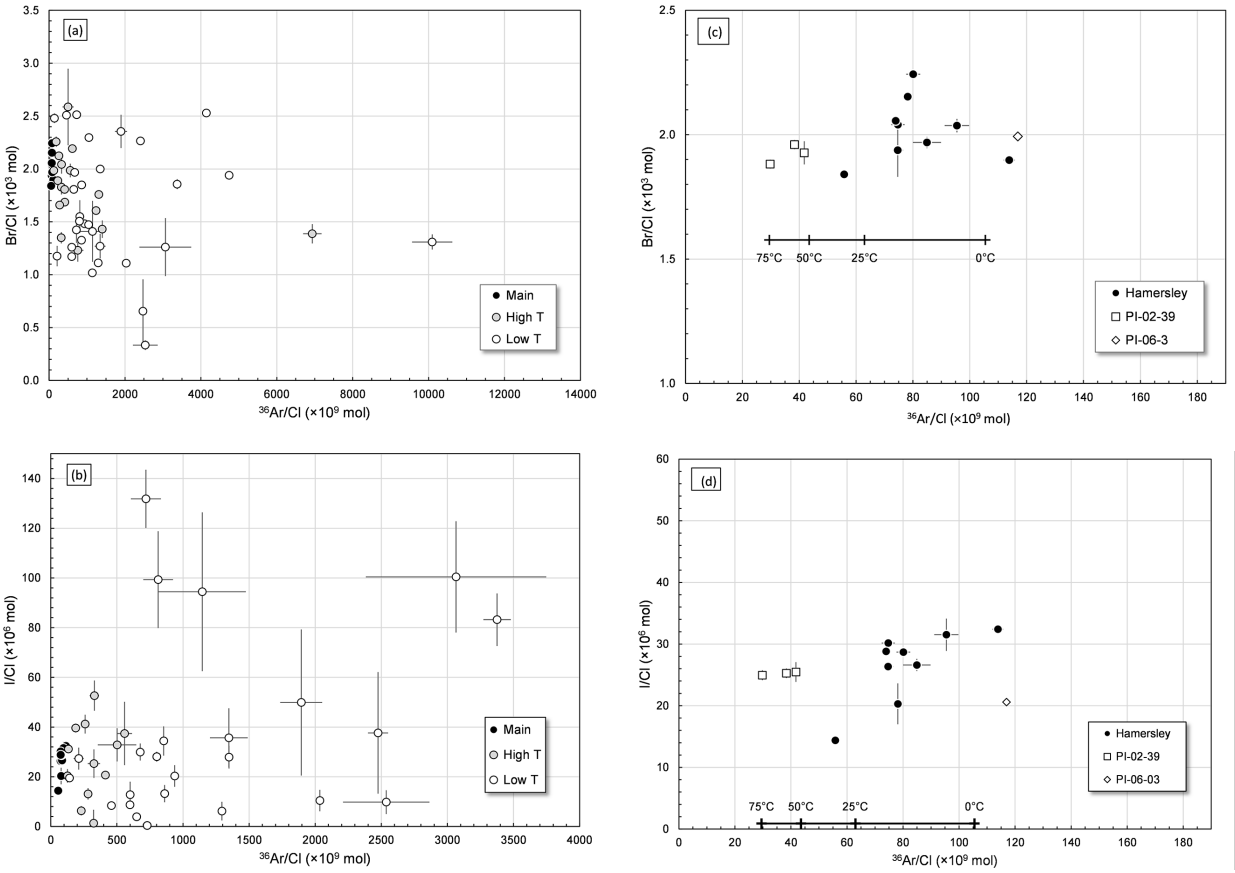

Figure 4. I-Br-Cl-^{36}Ar relationships in Hamersley and North Pole samples. (**a**) Hamersley data only showing decreasing scatter with increasing temperature steps. Symbols are defined in Figure 2. (**b**) Expanded scale showing the main release step for the Hammersley cherts and total crushing release from North Pole (PI) quartz samples. The solid horizontal lines represent modern seawater salinity over the temperature range 0–75 °C calculated using equations from Hamme and Emerson (2004).

of the halogens. There is considerable uncertainty about rates of deposition of BIF, with rates possibly differing between band types due to changes in clastic input. Sedimentation rates for the Dales Gorge Member have been estimated at 3–1000 m/Ma (Arndt et al. 1991; Barley et al. 1997; Martin et al. 1993; Trendall 2000; Trendall et al. 2004), meaning 1 cm of BIF represents 10–3000 yr of deposition. Note, these rates are not based on wet sediment deposition that would have been much higher, but instead on consolidated core that would have undergone approximately 95% compaction (see Trendall and Blockley 1970). Regardless of the high uncertainty, the suggested rates are orders of magnitude lower than the residence times of Cl, Br, and I in modern oceans of 1.1×10^8, 1.2×10^8, and 3.1×10^5 years, respectively (Martin and Whitfield 1983).

North Pole crushing gives Br/Cl values 1.9–2.0 × 10^{-3} M that are just above the range of 1.5–1.6 × 10^{-3} M obtained from two samples by crush leach analysis reported by Foriel et al. (2004). The minor disparity may reflect a higher proportion of hydrothermal fluid contributing to our determination, or perhaps be related to analytical differences between the techniques employed, e.g., crush leach may partially dissolve minor solid phases not sampled during noble gas crushing, or the noble gas technique may be biased toward release from larger inclusions having subtly different composition. Using synchrotron microanalysis, Foriel et al. (2004) determined Br/Cl values for individual fluid inclusions in North Pole quartz and found the composition of a low-metal bearing fluid to be similar to the bulk crush leach values. They interpreted this fluid type as being most representative of North Pole seawater on the basis having Br/Cl ratios similar to modern seawater values.

Halogen ratios of the ancient oceans: Biological and mantle influences

Based on the preceding discussion, halogens released at high temperature from Hamersley cherts, and during crushing release of North Pole quartz provide similar estimates for Br/Cl and I/Cl ratios of seawater for the time periods 2.5 and 3.5 Ga, respectively. Figure 5 plots I/Cl vs. Br/Cl for samples studied here, together with previously reported values of Archean seawater composition. Data from this study are reasonably consistent with previous values, although a comparison of I/Cl is only possible for Barberton (Channer et al. 1997), assuming the ironstone pods at Barberton are of Archean age, which is disputed (Lowe and Byerly 2003, 2007; Hren et al. 2006). The range of halogen ratios of Archean seawater are distinct from the modern mantle and chondrite values, which has relevance for understanding the distribution of halogens in the early Earth. Estimates suggest that 80–90% of terrestrial

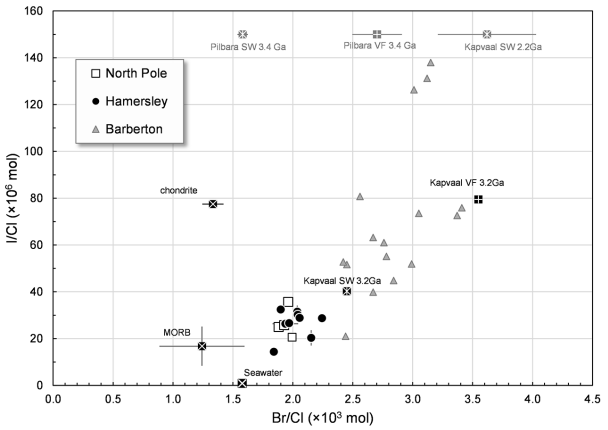

Figure 5. I/Cl vs. Br/Cl plot for Hamersley chert and North Pole quartz samples. Data and end-member (SW = seawater; VF = vent fluid) estimates for Barberton, Kapvaal are from Channer et al. (1997); de Ronde et al. (1997). Gray symbols at top of the graph are Br/Cl data only: Pilbara SW and VF = Foriel et al. (2004); Kapvaal SW = Gutzmer et al. (2003). Reference values are mid-ocean ridge basalts (MORB, representative of the Earth's depleted mantle) = Kendrick et al. (2017), chondrite meteorites = Clay et al. (2017), and modern seawater = (Li 1991).

Cl, Br, and I are currently stored in surface reservoirs (Burgess et al. 2002; Kendrick et al. 2017), significantly higher compared to the ~50% mantle degassing of noble gases. To account for these differences, Clay et al. (2017) argued that halogens were degassed in a large pulse, probably early in terrestrial evolution, and then stabilized in fluid or solid phases to avoid the extreme early loss processes experienced by noble gases (Pepin and Porcelli 2006). In this scenario, the early oceans would be expected to have chondrite-like halogen ratios. However, the estimates shown in Figure 5 indicate that seawater halogen chemistry had already evolved from this initial state by 3.5 Ga.

Higher plume activity, production of voluminous mafic crust (Smithies et al. 2005), higher outgassing rates (Sleep and Zahnle 2001) and increased vigour of high-temperature hydrothermal activity (Shibuya et al. 2007) means there was probably a stronger connection between the mantle and ocean chemistry during the Archean. The halogen composition of the Archean mantle is unknown, and in modern seafloor hydrothermal systems Br/Cl ratios are not usually fractionated from mantle values by >10% during boiling and phases separation processes (see Kendrick 2018 for review). Higher than mantle Br/Cl ratios, similar to those estimated for Archean hydrothermal fluids (Channer et al. 1997; Gutzmer et al. 2003; Foriel et al. 2004; Farber et al. 2015) are present in fluids in hydrothermally altered ocean crust and may be explained by mixing of seawater ± mantle halogens followed by fractionation of Br and Cl during amphibole crystallization during high-temperature ocean crust alteration (Kendrick et al. 2015; Chavrit et al. 2016). In contrast to seafloor alteration processes that do not strongly affect the Br/Cl ratios, organic matter fractionates Cl and Br, and the lack of a significant organic reservoir was proposed to explain the high Br/Cl of Palaeoproterozoic seawater (Gutzmer et al. 2003).

An Archean marine reservoir of iodine much larger than today's has previously been suggested based on the absence of, or more limited, biological control (de Ronde et al. 1997; Hardisty et al. 2014). The main iodine sink in the modern ocean is biological assimilation and burial in organic-rich marine sediments (Price and Calvert 1973; Price 1977; Muramatsu and Wedepohl 1998). In particular, marine algae accumulate iodine (and some bromine) with a concentration factor from seawater of around five orders of magnitude (and up to one order of magnitude for Br; Küpper et al. 2013). Most of the organically bound iodine is released back to into seawater during the decomposition of organic matter (Ullman and Aller 1980, 1983). Under anoxic conditions, which characterized early Archean oceans, seawater iodate is reduced to iodide, which adsorbs less readily on to organic matter making burial of iodine less efficient (Zhou et al. 2015). This is because in contrast to seafloor alteration processes that do not affect the Cl/Br ratios, organic matter fractionates Cl and Br. Overall, the relatively small iodine sink of sedimentary organic matter predicted for the Archean, is supported by our finding of I/Cl ratios much higher than the modern value.

Implications

This study addresses the Br/Cl and I/Cl composition of Archean and Palaeoproterozoic seawater by applying the noble gas neutron irradiation technique to chert and hydrothermal quartz samples. In addition to low detection levels for halogens, this technique has the potential advantage of being able to distinguish between primary and secondary components and provide age constraints on the timing of fluid entrapment. This is the first study to assess the potential of BIF cherts for reconstructing ancient seawater halogen compositions. Cherts containing preserved seawater exhibit the following characteristics: ^{36}Ar/Cl values consistent with the range predicted for ocean water salinity and temperature; ^{40}Ar-^{39}Ar ages that are equivalent to the chert depositional age; presence of paleoatmospheric noble gases dissolved in the seawater component; and high temperature (≥1400 °C) co-release of these attributes during melting of the host chert. Although the hydrothermal quartz and BIF chert formed in different depositional environments at separate times, they nonetheless trapped seawater with similar halogen ratios (Br/Cl ~ 2×10^{-3} M and I/Cl ~ 30×10^{-6} M).

The strong affinity of I for organic matter makes this element a sensitive tracer for the evolution of biological activity in the ocean and is particularly influenced by marine algae. The Archean ocean I/Cl value is intermediate between the bulk Earth (represented by chondritic meteorites) and modern seawater consistent with a smaller organic iodine reservoir in the Archean and Paleoproterozoic. The Br/Cl value of ancient seawater is elevated above modern seawater and chondritic values, and the cause of this is not understood. However, given the likely buffering of seawater halogen ratios by mantle inputs, it is suggested this may reflect stronger Br and Cl fractionation during seafloor hydrothermal processes relative to the modern day.

Acknowledgments and funding

We thank Zunli Lu and an anonymous reviewer for constructive reviews, and Anita Cadoux for editorial assistance. S.G. acknowledges funding from a NERC Ph.D. studentship that supported the analyses of the Hamersley chert samples. R.B. is grateful for a JSPS Fellowship that funded his stay at the University of Tokyo during which the manuscript was prepared.

References cited

Arndt, N.T., Nelson, D.R., Compston, W., Trendall, A.F., and Thorne, A.M. (1991) The age of the Fortescue Group, Hamersley Basin, Western Australia, from ion microprobe zircon U-Pb result. Australian Journal of Earth Sciences, 38, 261–281.

Avice, G. Marty, B., Burgess, R., Hofmann, A., Philippot, P., Zahnle, K., and Zakharov, D. (2018) Evolution of atmospheric xenon and other noble gases inferred from Archean to Paleoproterozoic rocks. Geochimica et Cosmochimica Acta, 232, 82–100.

Ballentine, C.J., Burgess, R., and Marty, B. (2002) Tracing fluid origin, transport and interaction in the crust. Reviews in Mineralogy and Geochemistry, 47, 539–614.

Barley, M.E., Pickard, A.L., and Sylvester, P.J. (1997) Emplacement of a large igneous province as a possible cause of banded iron formation 2.45 billion years ago. Nature, 385, 55–58.

Bohlke, J.K., and Irwin, J.J. (1992a) Laser microprobe analysis of Cl, Br,I and K in fluid inclusions: Implications for sources of salinity in some ancient hydrothermal fluids. Geochimica et Cosmochimica Acta, 56, 203–225.

——— (1992b) Laser microprobe analyses of noble gas isotopes and halogens in fluid inclusions: Analyses of microstandards and synthetic inclusions in quartz. Geochimica et Cosmochimica Acta, 56, 187–201.

Brown, M.C., Oliver, N.H.S., and Dickens, G.R. (2004) Veins and hydrothermal fluid flow in the Mt Whaleback Iron Ore District, eastern Hamersley Province, Western Australia. Precambrian Research, 128, 441–474.

Buick, R., and Dunlop, J.S.R. (1990) Evaporitic sediments of early Archaean age from the Warrawoona Group, North Pole, Western Australia. Sedimentology, 37, 247–277.

Burgess, R., Layzelle, E., Turner, G., and Harris, J.W. (2002) Constraints on the age and halogen composition of mantle fluids in Siberian coated diamonds. Earth and Planetary Science Letters, 197, 193–203.

Channer, D.M.D., de Ronde, C.E.J., and Spooner, E.T.C. (1997) The Cl^--Br^--I^- composition of ~3.23 Ga modified seawater: Implications for the geological evolution of ocean halide chemistry. Earth and Planetary Science Letters, 150, 325–335.

Chavrit, D., Burgess, R., Sumino, H., Teagle, D.A.H., Droop, G., Shimizu, A., and Ballentine, C.J. (2016) The contribution of hydrothermally altered ocean crust to the mantle halogen and noble gas cycles. Geochimica et Cosmochimica Acta, 183, 106–124.

Clay, P.L., Burgess, R., Busemann, H., Ruzié-Hamilton, L., Joachim, B., Day, J.M.D., and Ballentine, C.J. (2017) Halogens in chondritic meteorites and terrestrial accretion. Nature, 551, 614–618.

de Ronde, C.E.J., Channer, D.M.de, R., Faure, K., Bray, C.J., and Spooner, E.W.C. (1997) Fluid chemistry of Archean seafloor hydrothermal vents: Implications for the composition of circa 3.2 Ga seawater. Geochimica et Cosmochimica Acta, 61, 4025–4042.

de Ronde, C.E.J., De Wit, M.J., Spooner, E.T.C., Channer, D.M.deR., Christenson, B.W., Bray, C.J., and Faure, K. (2004) Ironstone pods in the Archean Barberton greenstone belt, South Africa: Earth's oldest seafloor hydrothermal vents reinterpreted as Quaternary subaerial springs: Comment and Reply. Geology, 32, Online Forum, e68–e69.

Egglseder, M.S., Cruden, A.R., Tomkins, A.G., Wilson, S.A., and Langendam, A.D. (2018) Colloidal origin of microbands in banded iron formations. Geochemical Perspectives Letters, 6, 43–49.

Ewers, W.E., and Morris, R.C. (1981) Studies of the Dales Gorge Member of the Brockman Iron Formation, Western Australia. Economic Geology, 76, 1929–1953.

Farber, K., Dziggel, A., Meyer, F.M., Prochaska, W., Hofmann, A., and Harris, C. (2015) Fluid inclusion analysis of silicified Palaeoarchaean oceanic crust—A record of Archaean seawater? Precambrian Research, 266, 150–164.

Foriel, J., Philippot, P., Rey, P., Somogyi, A., Banks, D., and Menez, B. (2004) Biological control of Cl/Br and low sulfate concentration in a 3.5 Gyr-old seawater from North Pole, Western Australia. Earth and Planetary Science Letters, 228, 451–463.

Gutzmer, J., Banks, D.A., Luders, V., Hoefs, J., Beukes, N.J., and von Bezing, K.L. (2003) Ancient sub-seafloor alteration of basaltic andesites of the Ongeluk Formation, South Africa: Implications for the chemistry of Paleoproterozoic seawater. Chemical Geology, 201, 37–53.

Hamade, T. (2002) Chemical fluctuation in Precambrian banded iron formations. Ph.D. thesis, University of Leeds, U.K.

Hamade, T., Konhauser, K.O., Raiswell, R., Goldsmith, S., and Morris, R.C. (2003) Using Ge/Si ratios to decouple iron and silica fluxes in Precambrian banded iron formations. Geology, 31, 35–38.

Hamme, R.C., and Emerson, S.R. (2004) The solubility of neon, nitrogen and argon in distilled water and seawater. Deep Sea Research Part I: Oceanography Research Papers, 51, 1517–1528.

Hardisty, D.S., Lu, Z., Planavsky, N.J., Bekker, A., Philippot, P., Zhou, X., and Lyons, T.W. (2014) An iodine record of Paleoproterozoic surface ocean oxygenation. Geology, 42, 619–622.

Hren, M.T., Lowe, D.R., Tice, M.M., Byerly, G., and Chamberlain, C.P. (2006) Stable isotope and rare earth element evidence for recent ironstone pods within theArchean Barberton greenstone belt, South Africa. Geochimica et Cosmochimica Acta, 70, 1457–1470.

Kamber, B.S., Greig, A., and Collerson, K.D. (2005) A new estimate for the composition of weathered young upper continental crust from alluvial sediments, Queensland, Australia. Geochimica et Cosmochimica Acta, 69, 1041–1058.

Kaufman, A.J., Hayes, J.M., and Klein, C. (1990) Primary and diagenetic controls of isotopic compositions of iron-formation carbonates. Geochimica et Cosmochimica Acta, 54, 3461–3473.

Kelley, S., Turner, G., Butterfield, A.W., and Shepherd, T.J. (1986) The source and significance of argon isotopes in fluid inclusions from areas of mineralization: Earth and Planetary Science Letters, 79, 303–318.

Kendrick, M.A. (2012) High precision Cl, Br and I determinations in mineral standards using the noble gas method. Chemical Geology, 292-293, 116–126.

——— (2018) Halogens in seawater, marine sediments and the altered oceanic lithosphere. In D.E. Harlov and L. Aranovich, Eds., The Role of Halogens in Terrestrial and Extraterrestrial Geochemical Processes, p. 591–648. Springer Geochemistry.

Kendrick, M.A., Burgess, R., Pattrick, R.A.D., and Turner, G. (2001) Halogen and Ar–Ar age determinations of inclusions within quartz veins from porphyry copper deposits using complementary noble gas extraction techniques. Chemical Geology, 177, 351–370.

Kendrick, M.A., Honda, M., and Vanko, D.A. (2015) Halogens and noble gases in Mathematician Ridge metagabbros: Implications for oceanic hydrothermal root zones and global volatile cycles. Contributions in Mineralogy and Petrology, 170, 1–20.

Kendrick, M.A., Hémond, C., Kamenetsky, V.S., Danyushevsky, L., Devey, C.W., Rodemann, T., Jackson, M.G., and Perfit, M.R. (2017) Seawater cycled throughout Earth's mantle in partially serpentinized lithosphere. Nature Geoscience, 10, 222–228.

Knauth, L.P. (1998) Salinity history of the Earth's early ocean. Nature, 395, 554–555.

Knauth, L.P., and Lowe, D.R. (2003) High Archean climatic temperature inferred from oxygen isotope geochemistry of cherts in the 3.5 Ga Swaziland Supergroup, South Africa. Geological Society of America Bulletin, 115, 566–580.

Konhauser, K.O., Planavsky, N.J., Hardisty, D.S., Robbins, L.J., Warchola, T.J., Haugaard, R., Lalondee, S.V., Partin, C.A., Oonk, P.B.H., Tsikos, H., and others. (2017) Iron formations: A global record of Neoarchaean to Palaeoproterozoic environmental history. Earth Science Reviews, 172, 140–177.

Krapež, B., Barley, M.E., and Pickard, A.L. (2003) Hydrothermal and resedimented origins of the precursor sediments to banded iron formations: Sedimentological evidence from the early Palaeoproterozoic Brockman Supersequence of Western Australia. Sedimentology, 50, 979–1011.

Küpper, F.C., Carpenter, L.J., Leblanc, C., Toyama, C., Uchida, Y., Maskrey, B.H., Robinson, J., Verhaeghe, E.F., Malin, G., Luther, G.W. III, and others. (2013) In vivo speciation studies and antioxidant properties of bromine in Laminaria digitata reinforce the significance of iodine accumulation for kelps. Journal of Experimental Botany, 64, 2653–2664.

Li, Y.-H. (1991) Distribution patterns of the elements in the ocean: A synthesis. Geochimica et Cosmochimica Acta, 55, 3223–3240.

Lowe, D.R., and Byerly, G.R. (2003) Ironstone pods in the Archean Barberton greenstone belt, South Africa: Earth's oldest seafloor hydrothermal vents reinterpreted as Quaternary subaerial springs. Geology, 31, 909–912.

——— (2004) Ironstone pods in the Archean Barberton greenstone belt, South Africa: Earth's oldest seafloor hydrothermal vents reinterpreted as Quaternary subaerial springs: Reply. Geology, 32, Online Forum, e69.

——— (2007) Ironstone bodies of the Barberton greenstone belt South Africa: products of a Cenozoic hydrological system, not Archean hydrothermal vents! Geological Society of America Bulletin, 119, 65–87.

Maliva, R.G., Knoll, A.H., and Simonson, B.M. (2005) Secular change in the Precambrian silica cycle: insights from chert petrology. Geological. Society America Bulletin, 117, 835–845.

Martin, J.-M., and Whitfield, M. (1983) The significance of the river input of chemical elements to the ocean. In C.S. Wong, E. Boyle, K.W. Bruland, J.D. Burton, and E.D. Goldberg, Eds., Trace Metals in Seawater, p. 265–296. Plenum Press, New York.

Martin, J.B., Gieskes, J.M., Torres, M., and Kastner, M. (1993) Bromine and iodine in Peru margin sediments and pore fluids: Implications for fluid origins. Geochimica et Cosmochimica Acta, 57, 4377–4389.

Martin, H., Claeys, P., Gargaud, M., Pinti, D., and Selsis, F. (2006) 6. Environmental context. Earth, Moon, and Planets, 98, 205–245. Springer.

Marty, B., Zimmermann, L., Pujol, M., Burgess, R., and Philippot, P. (2013) Nitrogen isotopic composition and density of the Achaean atmosphere. Science, 342, 101–104.

Marty, B., Avice, G., Bekaert, D.V., and Broadley, M.W. (2018) Salinity of the Archaean oceans from analysis of fluid inclusions in quartz. Comptes Rendus Geoscience, 350, 154–163.

Moran, J.E., Oktay, S.D., and Santschi, P.H. (2002) Sources of iodine and iodine 129 in rivers. Water Resources Research, 38, 1149–1158.

Morris, R.C. (1993) Genetic modelling for banded iron-formation of the Hamersley Group, Pilbara craton, Western Australia. Precambrian Research, 60, 243–286.
Muramatsu, Y., and Wedepohl, K.H. (1998) The distribution of iodine in the Earth's crust. Chemical Geology, 147, 201–216.
Pecoits, E., Gingras, M.K., Barley, M.E., Kappler, A., Posth, N.R., and Konhauser, K.O. (2009) Petrography and geochemistry of the Dales Gorge banded iron formation: Paragenetic sequence, source and implications for palaeo-ocean chemistry. Precambrian Research, 172, 163–187.
Pepin, R.O., and Porcelli, D. (2006) Xenon isotope systematics, giant impacts, and mantle degassing on the early Earth. Earth and Planetary Science Letters, 250, 470–485.
Pinti, D.L., Hashizume, K., Sugihara, A., Massault, M. and Philippot, P. (2009) Isotopic fractionation of nitrogen and carbon in Paleoarchean cherts from Pilbara craton, Western Australia: origin of ^{15}N-depleted nitrogen. Geochimica et Cosmochimica Acta, 73, 3819–3848.
Posth, N.R., Hegler, F., Konhauser, K.O., and Kappler, A. (2008) Alternating Si and Fe deposition caused by temperature fluctuations in Precambrian oceans. Nature Geoscience 1, 703–708.
Price, N.B. (1977) The contrasting geochemical behaviours of iodine and bromine in Recent sediments from the Namibian shelf. Geochimica et Cosmochimica Acta, 41, 1769–1775.
Price, N.B., and Calvert, S.E. (1973) The geochemistry of iodine in oxidized and reduced recent marine sediments. Geochimica et Cosmochimica Acta, 37, 2149–2158.
Pujol, M., Marty, B., and Burgess, R. (2011) Chondritic-like xenon trapped in Archean rocks: A possible signature of the ancient atmosphere. Earth and Planetary Science Letters, 308, 298–306.
Pujol, M., Marty, B., Burgess, R., Turner, G., and Philippot, P. (2013) Argon isotopic composition of Archean atmosphere probes early Earth geodynamics. Nature, 498, 87–90.
Rasmussen, B., Fletcher, I.R., and Sheppard, S. (2005) Isotopic dating of the migration of a low-grade metamorphic front during orogenesis. Geology, 33, 773–776.
Rasmussen, B., Meier, D.B., Krapež, B., and Muhling, J.R. (2013) Iron silicate microgranules as precursor sediments to 2.5 billion-year-old banded iron formations. Geology, 41, 435–438.
Rasmussen, B., Krapež, B., and Meier, D.B. (2014) Replacement origin for hematite in 2.5 Ga banded iron formation: evidence for postdepositional oxidation of iron-bearing minerals. Geological Society of America Bulletin, 126, 438–446.
Robbins, L.J., Funk, S., Flynn, S.L., Warchola, T.J., Li, Z., Lalonde, S.V., Rostron, B.J., Smith, J.B., Beukes, N.J., de Kok, M.O., and others. (2019) Hydrogeological constraints on the formation of Palaeoproterozoic banded iron formations. Nature Geoscience, 12, 558–563.
Ruzié-Hamilton, L., Clay, P., Burgess, R., Joachim, B., Ballentine, C., and Turner, G. (2016) Determination of halogen abundances in terrestrial and extraterrestrial samples by the analysis of noble gases produced by neutron irradiation. Chemical Geology, 437, 77–87.
Saiz-Lopez, A., Plane, J.M.C., Baker, A.R., Carpenter, L.J., von Glasow, R., Gomez Martín, J.C., McFiggans, G., and Saunders, R.W. (2012) Atmospheric chemistry of iodine. Chemical Reviews, 112, 1773–1804.
Schopf, J.W., Kudryavtsev, A.B., Agresti, D.G., Wdoowiak, T.J., and Czaja, A.D. (2002) Laser-Raman imagery of Earth's earliest fossils. Nature, 416, 73–76.
Shibuya, T., Kitajima, K., Komiya, T., Terabayashi, M., and Maruyama, S. (2007) Middle Archean ocean ridge hydrothermal metamorphism and alteration recorded in the Cleaverville area, Pilbara Craton,Western Australia. Journal of Metamorphic Geology, 25, 751–767.
Sleep, N.H., and Zahnle, K.J. (2001) Carbon dioxide cycling and implications for climate on ancient Earth. Journal of Geophysical Research, 106, 1373–1399.
Smith, R.E., Perdrix, J.L., and Parks, T.C. (1982) Burial metamorphism in the Hamersley Basin, Western Australia. Journal of Petrology, 23, 75–102.
Smithies, R.H., Van Kranendonk, M.J., and Champion, D.C. (2005) It started with a plume—early Archaean basaltic proto-continental crust. Earth and Planetary Science Letters, 238, 284–297.
Stuart, F., Turner, S., and Taylor, R. (1994) He-Ar isotope systematics of fluid inclusions: Resolving mantle and crustal contributions to hydrothermal fluids. In J. Matsuda, Ed., Noble Gas Geochemistry and Cosmochemistry, p. 261–277. Terra Scientific Publishing Company, Tokyo.
Svensen, H., Jamtveit, B., Banks, D., and Austrheim, H. (2001) Halogen contents of eclogite facies fluid inclusions and minerals: Caledonides, western Norway. Journal of. Metamorphic Geology, 19, 165–178.
Sun, S., Konhauser, K.O., Kappler, A., and Yiliang, L. (2015) Primary hematite in Neoarchean to Paleoproterozoic oceans. Geological Society of America Bulletin, 127, 850–861.
Tagami, K., and Uchida, S. (2006) Concentrations of chlorine, bromine and iodine in Japanese rivers. Chemosphere, 65, 2358–2365.
Terabayashi, M., Masada, Y., and Ozawa, H. (2003) Archean ocean-floor metamorphism in the North Pole area, Pilbara Craton. Western Australia. Precambrian. Research, 127, 167–180.
Trendall, A.F. (2000) The significance of banded iron formation (BIF) in the Precambrian stratigraphic record. Geoscientist, 10, 4–7.
Trendall, A.F., and Blockley, J.G. (1970) The iron formations of the Precambrian Hamersley Group Western Australia with special reference to the associated crocidolite: Geological Survey of Western Australia Bulletin, 119, 1–366.
Trendall, A.F., Compston, W., Nelson, D.R., De Laeter, J.R., and Bennett, V.C. (2004) SHRIMP zircon ages constraining the depositional chronology of the Hamersley Group, Western Australia. Australian Journal of Earth Sciences, 51, 621–644.
Turner, G. (1965) Extinct iodine 129 and trace elements in chondrite. Journal of Geophysical Research, 70, 5433–5445.
——— (1988) Hydrothermal fluids and argon isotopes in quartz veins and cherts. Geochimica et Cosmochimica Acta, 52, 1443–1448.
——— (1989) The outgassing history of the Earth's atmosphere. Journal of the Geological Society, 146, 147–154.
Turner, G., Burnard, P.G., Ford, J.L., Gilmour, J.D., Lyon, I.C., and Stuart, F.M. (1993) Tracing fluid sources and interactions. Philosophical Transactions—Royal Society of London A, 344, 127–140.
Ullman, W.J., and Aller, R.C. (1980) Dissolved iodine flux from estuarine sediments and implications for the enrichment of iodine at the sediment water interface. Geochimica et Cosmochimica Acta, 44, 1177–1184.
——— (1983) Rates of iodine remineralization in terrigenous near-shore sediments. Geochimica et Cosmochimica Acta, 47, 1423–1432.
Van Kranendonk, M.J. (2006) Volcanic degassing, hydrothermal circulation and the flourishing of early life on Earth: A review of the evidence from ca. 3490–3240 Ma rocks of the Pilbara Supergroup, Pilbara Craton, Western Australia. Earth Science Reviews, 74, 197–240.
Van Kranendonk, M.J., Webb, G.E., and Kamber, B.S. (2003) Geological and trace element evidence for amarine sedimentary environment of deposition and biogenicity of 3.45 Ga stromatolitic carbonates in the Pilbara Craton, and support for a reducing Archaean ocean. Geobiology, 1, 91–108.
Weiershäuser, L., and Spooner, E.T.C. (2005) Seafloor hydrothermal fluids, Ben Nevis area Abitibi Greenstone Belt: implications for Archean (~2.7 Ga) seawater properties. Precambrian Research, 138, 89–123.
Zhou, X., Jenkyns, H.C., Owens, J.D., Junium, C.K., Zheng, X.-Y., Sageman, B.B., Hardisty, D.S., Lyons, T.W., Ridgwell, A., and Lu Z. (2015) Upper ocean oxygenation dynamics from I/Ca ratios during the Cenomanian-Turonian OAE 2. Paleoceanography, 30, 510–526.

Manuscript received July 31, 2019
Manuscript accepted February 14, 2020
Manuscript handled by Anita Cadoux

Endnote:

[1]Deposit item AM-20-97238, Supplemental Material. Deposit items are free to all readers and found on the MSA website, via the specific issue's Table of Contents (go to http://www.minsocam.org/MSA/AmMin/TOC/2020/Sep2020_data/Sep2020_data.html).